Temporal and spatial dynamics in the apple flower microbiome in the presence of the phytopathogen *Erwinia amylovora*

Running title: Flower microbiome dynamics with a phytopathogen

Zhouqi Cui[1], Regan B. Huntley[1], Quan Zeng[1*], and Blaire Steven[2*]

[1]Department of Plant Pathology and Ecology, The Connecticut Agricultural Experiment Station, New Haven, Connecticut, 06504 USA;

[2] Department of Environmental Sciences, The Connecticut Agricultural Experiment Station, New Haven, Connecticut, 06504 USA

* Corresponding author: Blaire Steven. Email: blaire.steven@ct.gov; Quan Zeng. Email: quan.zeng@ct.gov

Abstract:

Plant microbiomes have important roles in plant health and productivity. However, despite flowers being directly linked to reproductive outcomes, little is known about the microbiomes of flowers and their potential interaction with pathogen infection. Here, we investigated the temporal dynamics and spatial traits of the apple stigma microbiome when challenged with a phytopathogen *Erwinia amylovora*, the causal agent of fire blight disease. We profiled the microbiome from the stigmas of a single flower, greatly increasing the resolution at which we can characterize shifts in the composition of the microbiome. Individual flowers harbored unique microbiomes at the OTU level. However, taxonomic analysis of community succession showed a population gradually dominated by bacteria within the families *Enterobacteriaceae* and *Pseudomonadaceae*. Flowers inoculated *E. amylovora* established large populations of the phytopathogen, with pathogen specific gene counts of $>3.0 \times 10^7$ in 90% of the flowers. Yet, only 42% of inoculated flowers later developed fire blight symptoms. This reveals pathogen amount on the stigma is not sufficient to predict disease outcome. Our data demonstrate that apple flowers represent an excellent model in which to characterize how plant microbiomes establish, develop, and interact with biological processes such as disease progression in an experimentally tractable plant organ.

Introduction

Flowers, the reproductive organs of angiosperms, play a critical role in the plant's lifecycle. The most important function of flowers is to provide a mechanism for pollination, the union of sperm contained within pollen, to the ovules contained in the ovary. The fertilized ovules produce seeds that will later germinate to become the next generation of plants. Yet, unlike other vegetative organs such as the roots, stems, and leaves that are present through a large part of the plant's lifecycle, flowers develop on mature plants and are typically present for the limited period during bloom. As such, research characterizing the microbiome of the flower is generally less developed than for other plant organs.

Flowers of apple (*Malus domestica*) have been subject to considerable research attention as they are the direct precursors of apple fruits, one of the most consumed fruits worldwide (1). The ephemeral nature of apple flowers, with mature flowers from petal open to petal fall only lasting for 5-10 days in spring, offers a unique environment in which to study community succession (1, 2). During bloom, petals open up in a relatively short period of time, typically within one day, which exposes the internal flower parts to the environment and microorganisms. Several of these internal flower parts exude various types of nutrient-rich secretions including nectar, stigmatic exudate, and pollen exudate, for the purpose of attracting pollinators, and inducing the germination of pollen grains (1, 3). These secretions are rich in sugars, amino acids, polysaccharides, and glycoproteins, which are excellent sources of nutrients for many microorganisms (1, 3, 4). The stigma is particularly nutrient rich and harbors a larger microbial biomass than other flower parts (5, 6). Previous research has documented a relatively low diversity of the stigma

63 microbiome, although certain lineages predominantly within the families
64 *Enterobacteriaceae* and *Pseudomonadaceae* tend to be dominant (7).

65 While the stigma provides an excellent niche for microbial colonization, it also
66 offers an opportunity for pathogen infection. Many pathogens have evolved to take
67 advantage of this environmental niche, among which one of the most important is the
68 phytopathogenic bacterium *Erwinia amylovora*, the causal agent of fire blight. Fire blight
69 is considered as one of the most devastating diseases of apple, with annual losses and
70 costs of control estimated at over $100 million in the U.S. (8). During bloom, *E.*
71 *amylovora* (*Ea*) cells are spread to apple flowers by insects, wind, or rain and multiply on
72 the stigma surface (9). *Ea* cells can then migrate from the stigma to the hypanthium and
73 enter into the host through the natural opening, the nectarthodes. Initial infection occurs
74 at the ovary tissue and can spread to other parts of the plants through the plant
75 vasculature system. Fire blight infection can result in significant yield reduction and / or
76 tree death. In this regard, uncovering environmental or biologic factors that can inhibit
77 the spread or development of fire blight are of considerable research interest.

78 One potential source of fire blight control is the natural microbiome of the stigma.
79 Yet, there exist considerable knowledge gaps concerning how the stigma microbiome is
80 established and structured. The studies that have considered the stigma microbiome have
81 generally focused on cataloging microbial diversity through various culture-dependent
82 and culture-independent methods (7, 10) and few studies have investigated the temporal
83 development of the microbiome (2). Furthermore, previous research has predominantly
84 studied the microbiome using pooled flower samples, thus it is uncertain the extent to
85 which the microbiome differs among individual flowers of the same genetic background.

Finally, how the colonization of a phytopathogen affects the development, composition, or structure of the stigma microbiome is essentially unknown. In this study, we examined the temporal development of the stigma microbiome in the presence and absence of *Ea* to investigate how this organism influences the development of the normal microflora of the apple flower stigma. Additionally, we characterized the variability of the microbiome amongst 100 individual stigmas inoculated with *Ea* to assess if certain microbiome members could regulate *Ea* colonization and growth on apple stigmas.

Materials and methods

Sampling site

To limit the effects of host and environmental conditions, we used flowers from nine trees of the same apple cultivar 'Early Macoun' (*Malus domestica* NY75414-1) planted at the same geographical location (Lockwood Farm, Hamden, Connecticut, 41.406 N 72.906 W). All trees were the same age and under the same maintenance program. Weather data (temperature and humidity) prior to and during bloom (from April 29th to May 28th 2018) is summarized in Table S1.

Experiment design and stigma collection

Labeling flower clusters

On May 6th 2018, 40 flower clusters that were in 'King bloom' stage (central flower opened but the four side flowers still closed, see Fig. 1A) were labeled with plastic tags. The day after the flower clusters were tagged, we identified clusters in which the

side flowers were open and flower clusters with unopened flowers were not used. In this manner, only side flowers of roughly the same age were used in subsequent experiments.

Sampling for temporal alterations of the stigma microbiome

On May 7th 2018, ten of the 40 tagged flower clusters were selected, and the stigmas of an individual flower were harvested with sterile scissors (see Fig. 1B) and placed in a sterile 1.5 ml microcentrifuge tube. Collected stigma samples were kept in liquid nitrogen and transported to the laboratory for immediate processing. These samples were labeled as day 1 samples. The next day, another 10 flowers were selected for DNA extraction as described above (as day 2 samples). Immediately after sample collection on day 2, *Ea* was inoculated onto 20 tagged flower clusters and labeled as *Ea* treated. The inoculum consisted of an overnight culture of *E. amylovora* 110 grown in lysogeny broth (LB) diluted to a final concentration of 1 x 10^6 CFU ml^{-1} in sterile water. The diluted culture was spray-inoculated to the open flowers using a handheld sprayer to ensure every flower was evenly exposed. Another twenty flower clusters were sprayed with sterile water as water controls. On each subsequent day (day 3 to day 5), stigmas from 20 *Ea*-treated and 20 water-treated flowers were collected and processed according to the same method described above.

Sampling for spatial patterns in the stigma microbiome

To investigate a larger spatial sampling of *Ea* inoculated flowers, we performed a parallel experiment, and tagged an additional 150 flower clusters to ensure flowers used in the experiment were the same age as the rest of the experimental set. As described for

131 the temporal sampling, the flower clusters were individually spray-inoculated with *Ea* (1
132 x 10^6 CFU ml^{-1}) on day 2, and stigma samples of individual flowers were harvested on
133 day 4. A total of 100 flowers of the same developmental stage were harvested for DNA
134 extraction, while the remaining flowers of each flower cluster were left on the tree to
135 monitor disease development. Blossom blight symptoms, black withering and dying of
136 the remaining flowers (Fig. 1C), were evaluated two weeks after inoculation on May 24th,
137 2018. An illustrated scheme of both temporal and spatial sampling is shown in Fig. S1.
138
139 *DNA extraction and sequencing of bacterial 16S rRNA genes*
140 For extraction of bacterial DNA, 200 µl of 0.5x phosphate-buffered saline (PBS)
141 was added to each microcentrifuge tube containing stigma samples. Epiphytic microbes
142 were removed from the stigma by a 5-minute water bath sonication followed by a 30-
143 second vortex. DNA was extracted from the 200 µl of bacterial suspension by using the
144 DNeasy PowerSoil Kit (Qiagen, Hilden, Germany) according to manufacturer's
145 instructions. The amount of template DNA added in the PCR reaction (25 µl) ranged
146 from 10.0 ng to 20.0 ng as determined by Nanodrop2000 (Thermo Fisher Scientific,
147 Waltham, MA). DNA was amplified by using the 515f/806r primer set, which targets the
148 V4 region of the bacterial 16S rRNA gene, with both primers containing a 6-bp barcode
149 unique to each sample (11). PNA clamps were added to the PCR mixture at a
150 concentration of 0.75 µM to block the PCR amplification of apple plastid and
151 mitochondrial sequences (7). PCR conditions were performed as described in Steven et
152 al. (2018) (7). Successful PCR amplifications at the correct amplicon size were confirmed
153 by gel electrophoresis. The PCR products were purified and normalized by using

SequalPrep normalization plate kit (Invitrogen, CA, USA). Pyrosequencing was conducted on an Illumina MiSeq v2.2.0 platform through services provided by the UConn MARS facility.

Quantitative PCR for enumeration of E. amylovora

The abundance of *Ea* in each collected stigma sample was quantified by determining the cycle threshold (CT) value of the *Ea* specific gene *amsC* (12). Quantitative PCR (qPCR) was performed using a SsoAdvanced universal SYBR Green supermix (Bio-Rad, CA, USA), as described previously (13). The CT values for a 1/10 dilution series of known *amsC* gene copies of *E. amylovora* chromosomal DNA was determined to make a standard curve for calculation of copy numbers in stigma samples.

Bioinformatics and statistical analysis.

Illumina sequencing reads were assembled into contigs and quality screened by using mothur v1.39.5 as previously described (14). Sequences that were at least 253 bp in length, contained no ambiguous bases, and no homopolymers of more than 8 bp were used in the analysis. Chimeric sequences were identified by using the VSEARCH as implemented in mothur (15), and all potentially chimeric sequences were removed. To maintain a similar sampling effort between samples, samples with less than 10,000 sequences per sample were also removed. The resulting sequence counts per sample are presented in Table S2. Negative control (PCR using sterile H_2O as a template) was also included in both sequence datasets. The sequences data are deposited in the Sequence Read Archive under accession number PRJNA597302.

Sampling effort was normalized to the depth of the smallest sample and operational taxonomic units (OTUs) were defined at 100% sequence identity, employing the OptiClust algorithm in mothur (16). Taxonomic classification of sequences was performed with the Ribosomal Database Project (RDP) classifier against the SILVA v132 reference alignment in mothur (17, 18). Non-metric multidimensional scaling (NMDS) was used to visualize the pairwise distances among samples with Bray-Curtis distances in the Vegan package in R (19). Descriptive diversity statistics were calculated in mothur. The correlation between alpha diversity determined with the non-parametric Shannon's Diversity Index and *E. amylovora* abundance in each sample was generated with the ggplot2.0 package for R (20). Statistically significant differences in diversity statistics were identified with a one-way ANOVA and Tukey-Kramer post hoc test in the agricolae package in R.

Results

Temporal patterns in stigma microbial community assembly

We characterized the microbial community on stigmas collected from individual flowers, over a period of 5 days after petal opening, to investigate the temporal dynamics in community assembly and microbial succession on the stigma. Meanwhile, we included *Ea* inoculated stigmas to compare community succession in the presence of a phytopathogen. A total of 2 930 231 high-quality filtered sequences were obtained from 96 samples with the number of sequences ranging from 10 210 to 97 668 (Table S2). These sequences clustered into 46 809 OTUs (mean 222 per sample) at 100% sequence similarity.

At the phylum level, 24 phyla were detected. In both the water control and *Ea* inoculated datasets, the dominant phylum was *Proteobacteria* (94.3% of total sequences), followed by *Cyanobacteria* (3.6%), *Actinobacteria* (0.8%), *Firmicutes* (0.2%) and *Bacteroidetes* (0.2%). A temporal pattern was observed, in that phyla outside the *Proteobacteria* were most abundant in the early time points (days 1 and 2) accounting for 15% of sequences and decreasing to <1% at later time points (Fig. S2).

Given the dominance of *Proteobacteria*, these sequences were classified to deeper taxonomic ranks. Sixty-seven families were identified, with the majority belonging to the *Enterobacteriaceae* (average 70.0%, blue bars) and *Pseudomonadaceae* (26.2%, red bars in Fig. 2), with small contributions from *Moraxellaceae* (0.6%), *Beijerinckiaceae* (0.2%), unclassified *Gammaproteobacteria* (0.3%), *Burkholderiaceae* (0.3%) and *Xanthomonadaceae* (0.2%) (Fig. 2). Of note, both *Pseudomonadaceae* and *Enterobacteriaceae* gradually accounted for a larger proportion of the microbiome as time progressed in both water control and *Ea* inoculated datasets (Fig. 2). Yet, the average proportion of *Enterobacteriaceae* (the family to which *Ea* belongs) was higher in the *Ea* treated flowers compared to water control (89.7% versus 45.6% at day 5) (Fig. 2).

Abundance of Ea on individual flowers

We employed two methods to assess the abundance of *Ea* in the datasets, relative abundance of *Ea* sequences in the dataset and *Ea* copy numbers quantified by qPCR of an *Ea* specific gene. First, we identified an OTU in the dataset that had 100% sequence identity with the inoculated *Ea* strain (OTU1; Table S3). OTU1 was detected every day but not in all samples. On days 1 and 2, prior to the stigma treatments, OTU1 made up an

223 average of 4% and 6% of the microbiome sequences, respectively (filled bars in Fig. 2).
224 In the control water sprayed stigmas the proportion of OTU1 gradually increased from an
225 average of 2% of sequences on day 3 to 13% on day 4, finally making up an average of
226 24% of sequence on day 5. In contrast, the populations of OTU1 were larger in the *Ea*
227 treated stigmas. By day 3 OTU1 accounted for an average of 50% of the sequence
228 libraries, increasing to 86% on day 4 and ending at 94% of sequences on day 5, a 2.9-fold
229 increase in comparison to the controls (Fig. 2).

230 In addition, qPCR was performed to quantify the genome copies of *Ea* in each
231 stigma sample. As was observed for OTU1, *Ea* was identified across the dataset. In the
232 pretreated stigmas (days 1 and 2) the average copy number of *Ea* DNA were ~7.7×10^6
233 (Fig. 2). In the control datasets, the DNA copy number were similar on days 3 and 4 at
234 5.7×10^6 and 7.4×10^6, respectively, and increased to 1.5×10^7 on day 5 (Fig. 2). In the
235 *Ea* inoculated flowers the copy number of *Ea* on day 3 (one day after inoculation) was
236 similar to the control flowers, suggesting *Ea* had not yet established strong growth on the
237 stigma (Fig. 2). However, by day 4 the average abundance of *Ea* on the treated stigmas
238 reached 3.0×10^7, a 300% increase compared to the controls, and increased further on
239 day 5 reaching an average of 4.3×10^8, a 28-fold increase in comparison to the controls
240 (Fig. 2). Taken together, these data suggest that *Ea* may be naturally present in the
241 orchard, as it was commonly detected in the pretreated and control stigmas. Yet, the *Ea*
242 inoculation clearly benefited *Ea* colonization, which was readily apparent by day 5, three
243 days after the inoculation.

244

245 *Effects of Ea inoculation on community composition and diversity*

To test if *Ea* treatment had a significant effect on microbiome composition, we visualized the Bray-Curtis distances among samples of each dataset using NMDS. The samples clearly clustered due to *Ea* inoculation, which was confirmed by permutational multivariate ANOVA (P = 0.001) (Fig. 3A). Additionally, samples were also clustered based on days post-bloom (P = 0.001) (Fig. 3A). Diversity of the stigma communities was assessed by calculating the Shannon's Diversity index. For both control and *Ea* inoculated datasets there was a trend towards increased diversity in the early time points, which then decreased by days 4 and 5 (Fig. 3B). When the control and *Ea* inoculated datasets were combined to test the overall effect of pathogen presence on microbial diversity, there was no significant difference in diversity due to *Ea* treatment (p=0.109; Fig. 3B).

Collectively, these findings indicate that taxonomically diverse microbial populations initially colonize the stigma of the apple flower. Gradually, a community dominated by representatives of the *Pseudomonadaceae* and *Enterobacteriaceae* families outcompetes these populations and become the predominant community members (Fig. 2), which results in an overall decrease in diversity of the stigma microbial community (Fig. 3B &C). In the face of *Ea* challenge there is a significant shift in the composition of the microbial community (Fig. 3A). Yet, there is no significant effect on the diversity of the community as a whole in comparison to the control flowers (Fig. 3B).

The influence of Ea inoculation on 100 spatially separated flower clusters

The data for the temporal dynamics were based on a limited number of samples. To further explore the interaction of microbes when colonized by a phytopathogen, we

269 expanded the analysis to 100 spatially separated flower clusters (approximately 400
270 individual flowers) inoculated with *Ea*. Flowers were collected from the clusters for
271 microbiome characterization, while the remainder of the flowers were left on the tree to
272 monitor the rate of disease development. Three weeks after *Ea* inoculation, only 42.4% of
273 the flowers developed fire blight symptoms. Given that the genetic background of the
274 host, flower age, and pathogen exposure were all identical between the inoculated
275 flowers, and the trials were all performed in the same orchard and thus under the same
276 environmental conditions, these observations suggest that none of these factors are
277 sufficient to explain or predict disease occurrence at the single flower level.
278
279 *Genome copies of Erwinia amylovora*
280 We measured the *amsC* copy number from 100 individual flowers by qPCR. The
281 copy number varied from 1.3×10^4 to 3.7×10^{10}. The average was 4.4×10^9 (dashed line,
282 Fig. 4A) and the majority (90%) of stigmas harbored $> 3.0 \times 10^7$ gene copies of *Ea*,
283 which is similar to the average of day 4 inoculated flowers in the temporal dynamics
284 study. These results indicate most of the stigmas harbored large populations of *Ea*,
285 despite only a proportion of flowers later developing fire blight symptoms.
286
287 *Microbiome composition*
288 A total of 4 176 840 high-quality 16S rRNA gene sequences were recovered from
289 the 100 flowers, with the number of sequences ranging from 19 297 to 80 130 per
290 sample. After normalizing sampling to the smallest dataset, clustering produced 27 843

291 OTUs (mean 282 per sample) at 100% sequence similarity. The detailed information for
292 each dataset is presented in Table S2.

293 At the phylum level, 22 phyla were identified among the sequences. The most
294 abundant, *Proteobacteria*, ranged from 96.8% to 100% of recovered sequences, followed
295 by *Actinobacteria* (0-0.5%), *Cyanobacteria* (0-1.6%) and *Firmicutes* (0-1.5%) (Fig. S3).
296 Within the *Proteobacteria*, 59 families were identified and *Pseudomonadaceae* (red bar
297 in Fig. 4B) and *Enterobacteriaceae* (blue bar) were predominant (> 81.5% in each
298 sample). Notably, the proportion of *Pseudomonadaceae* and *Enterobacteriaceae*
299 significantly varied among the 100 samples, from 0.02% to 99.20% and from 0.45% to
300 99.97%, respectively (Fig. 4B).

301

302 *OTUs within the Pseudomonadaceae and Enterobacteriaceae*

303 Sequences within *Pseudomonadaceae* and *Enterobacteriaceae* were classified to
304 deeper taxonomic ranks to investigate if particular OTUs were associated with *Ea*
305 abundance. Of the 10 most abundant OTUs in the dataset, four belonged to the
306 *Pseudomonadaceae* and six to the *Enterobacteriaceae*, representing five different genera
307 (Table S3). By in large each flower harbored a unique microbiome composition, with
308 widely varying abundance of the predominant OTUs among the samples (Fig. 4C &D).
309 Furthermore, there was no observable pattern in specific OTUs being co-abundant in the
310 samples with a high relative abundance of *Pseudomonadaceae* (Fig. 4B &C). For
311 example, when we tested the correlation between the relative abundance of the most
312 abundant *Pseudomonadaceae*-related OTU (OTU5; Table S3) and the relative abundance
313 of *Pseudomonadaceae* in the dataset, the result showed no relationship ($R^2 = 0.26$, Fig.

S4). In other words, it was not a specific OTU that accounted for the high prevalence of the family *Pseudomonadaceae*. In contrast, OTU1 (100% sequence identity to *E. amylovora*; Table S3) tended to be highly abundant in samples with elevated counts of *Ea* (Fig. 4A &D). However, in those samples with low *Ea* counts a particular *Enterobacteriaceae* OTU was not predominant, suggesting that a specific OTU was not outcompeting *Ea* in those samples in which *Ea* was not well established.

Correlates of Ea abundance to metrics of the stigma microbiome

To test if there were any aspects in the community data that were predictive of *Ea* abundance we performed four correlational analyses. First, the most abundant OTU in the dataset (OTU1) shared 100% sequence identity with the inoculated *Ea* strain (Table S3). Therefore, we tested the correlation between the relative abundance of OTU1 and the *amsC* gene copy number of *Ea*, and thereby testing if the relative abundance of OTU1 was correlated to *Ea* absolute abundance (Fig. 5A). The result showed there was a positive relationship between the two metrics, with an $R^2 = 0.29$, suggesting a relationship but low explanatory power. Second, as shown in Fig. 4B, many of the stigmas maintained a large proportion of *Pseudomonadaceae* populations. We investigated if there was a predictive relationship between the relative abundance of the *Pseudomonadaceae* and the copy number of *Ea.* The relationship displayed in a negative pattern but again had a low predictive value ($R^2 = 0.26$, Fig. 5B). Thus, an increasing proportion of *Pseudomonadaceae* was not associated with a reduction of *Ea* colonization or abundance. Finally, we tested if *Ea* abundance was correlated to two different metrics of diversity of the stigma microbiome, Shannon's diversity index and the number of

337 recovered OTUs. In both cases there was no relationship between *Ea* abundance and
338 diversity (Fig. 5C &D). Thus, there was no apparent effect of *Ea* abundance on the
339 overall diversity of the stigma microbial communities.
340
341 **Discussion**
342 The apple flower microbiome has been previously recognized as an important
343 factor for plant health and as a potential source of biocontrol agents against plant
344 pathogens (1, 10, 21). Additionally, since the stigma is the major site of pollination and
345 supports the growth of a large microbial population, microbial growth on the stigma may
346 also influence pollination (22, 23). Thus, the stigma of a flower is a particularly important
347 plant tissue for studying the microflora that associate with plants. Yet, information
348 concerning the establishment, composition, and development of the microbiome on
349 flower stigmas, as well as the disturbance by the colonization of a phytopathogen, are
350 largely lacking. Previous studies have generally described the flower microbiome from
351 whole flowers or nectar (1, 2, 24). In this study, we present data based on collecting the
352 stigmas from a single flower, increasing both the temporal and spatial resolution at which
353 the microbiome can be characterized.

354 Temporal dynamics are important for understanding the evolution of microbial
355 communities (25-27). Shade et al. (2013) characterized the development of the
356 microbiome on pools of apple flowers under a management program of treating the
357 flowers with the antibiotic streptomycin to control fire blight. They found bacteria in the
358 phyla TM7 and *Deinococcus* were predominant and showed signals of ecological
359 successions with flower age (2). In our study, bacteria within the families

360 *Pseudomonadaceae* and *Enterobacteriaceae* were numerically dominant (Fig. 2), which
361 is more congruous with other studies of both the culture-dependent (10) and culture-
362 independent characterizations (7) of apple flower microbial populations. This discrepancy
363 is likely due to methodological differences between studies, or PCR biases induced by
364 different PCR primer and blocking pairs. In either case, both studies identified strong
365 signals of temporal patterns in how the microbiome is structured with flower age. The
366 data presented here points to a core microbiome that was gradually established on the
367 stigma predominantly composed of *Pseudomonadaceae* and/or *Enterobacteriaceae*
368 within the phylum *Proteobacteria* (Fig. 2). The succession of these families was
369 associated with a reduction of other bacterial taxa, such as the *Moraxellaceae,*
370 *Xanthomonadaceae,* and *Burkholderiaceae,* which were only present in the early stages
371 of bloom (Fig. 2). Concurrently, the later stages of bloom were associated with a lower
372 diversity, supporting the observation that a small number of taxa had monopolized the
373 stigma environment as the flower aged (Fig. 2). These observations are consistent with
374 the stigmas being open to colonization by numerous bacteria in the initial stages of
375 bloom. As the petals open, multiple bacteria carried by wind, dew or insects are
376 introduced to the stigma creating a diverse microbial population (9). However, with time
377 those bacteria best adapted to the stigma environment prevail and flourish. This is
378 analogous to other observations, that complex microbial communities inoculated into a
379 simple medium converge on a state similarly composed of bacteria in the families
380 *Pseudomonadaceae* and *Enterobacteriaceae,* a phenomenon referred to as “emergent
381 simplicity” (28). Thus, there may be conserved rules that govern the assembly of
382 microbial communities, with respect to niche adaptation (5, 6), and microbial competition

383 (29). Yet, predicting specific microbiome states of individuals or whether the factors that
384 govern community assembly are deterministic or stochastic still remain significant
385 knowledge gaps.

386 Inoculation of the flowers with *Ea* induced a significant shift in the structure of
387 the microbiome (Fig. 3A). The data indicated that the abundance of *Ea* did not alter
388 microbiome diversity (Fig. 5C &D), but *Ea* abundance may be negatively correlated with
389 the presence of other microbes, particularly within the family *Pseudomonadaceae* (Fig.
390 5B). Most notably 90% of inoculated flowers inhabited large counts of *Ea* ($> 3.0 \times 10^7$
391 gene copies) and a high relative abundance of sequences identical to the inoculated
392 pathogen (Fig. 4A &D), yet less than half of the flowers (42%) later developed fire blight
393 symptoms. As the stigma sampling for microbiome characterization is necessity
394 destructive, we cannot definitively link the status of the microbiome to disease
395 development. However, these data strongly point to the absolute abundance of *Ea* to be a
396 poor predictive measurement of disease occurrence. Thus, there must be another
397 bottleneck in fire blight disease development beyond *Ea* growth on the stigma. These
398 could include microclimate (30), antimicrobial compounds or yeasts in the nectar (10,
399 24), and host system sensing signals of high bacterial density (31). Yet, the observation
400 of a high carrier rate of a pathogen with low disease incidence is synonymous with
401 reports for many human pathogens. For instance, it is well established that 20-40% of the
402 population are asymptomatic persistent carriers of *Staphylococcus aureus,* with a further
403 70-90% of people considered transient carriers (32). Yet only a minority of people will
404 develop diseases such as sepsis, pneumonia, or osteomyelitis caused by *S. auerus*
405 infection (33, 34). Similar phenomenon are observed for *Cutibacterium acnes* as a

406 contributor to skin acne, which is also a major population in the healthy skin microbiome
407 (35). In this respect, the dynamics of *Ea* growth and fire blight development appear to
408 follow similar dynamics of other diseases, with a high carrier rate, but lower disease
409 incidence.

410

411 **Conclusion**

412 In this study we show that the apple flower stigma microbiome shares many
413 characteristics with other host microbiome systems. In the initial stages of stigma
414 colonization, the microbiome is temporally dynamic, which eventually settles into an
415 equilibrium community (Fig. 2). Similar dynamics have been found in mammalian
416 infants, fish, and soil (36-38). At the OTU level, individual flowers harbor largely unique
417 microbiomes (Fig. 4C &D), similar to vertebrates and insects (39-41). Despite the
418 diversity of the stigma microbiome at the OTU level (~200 OTUs per sample), the OTUs
419 fell into just two predominant families (*Pseudomonadaceae* and *Enterobacteriaceae*) that
420 differed in abundance between individual flowers (Fig. 2 &4). This mirrors the
421 observation of the dominance of the *Firmicutes* and *Bacteroidetes* in the human intestinal
422 tract, the so-called *Firmicutes/Bacteroidetes* ratio, and its potential influence on
423 characteristics such as obesity (42, 43). Finally, we observe that virtually all flowers
424 exposed to the phytopathogen *E. amylovora* developed large pathogen loads (Fig. 4), yet
425 only a fraction (~42%) of the flowers developed disease, reflecting a common
426 observation that pathogen burden is not always predictive of disease development (31,
427 44). Thus, we propose that the stigma microbiome is not only an important system to
428 potentially identify biocontrol agents for impeding the development of fire blight, but

represents a model system that can be employed to investigate the rules that govern microbial community assembly, development, and influence on disease progression and severity.

Conflict of Interests

The authors declare no conflict of interest.

Acknowledgments

We thank Sali Diallo and Zach Seltzer for their technical support. This study was supported by the USDA-NIFA-Organic Transitions grant 2017-51106-27001, Northeastern IPM Center partnership grant and USDA-Specialty Crop Block Grant (SCBG) through the Department of Agriculture, State of Connecticut.

Supplementary information is available at ISME's website.

Reference:

1. Aleklett K, Hart M, Shade A. The microbial ecology of flowers: an emerging frontier in phyllosphere research. Botany. 2014;92(4):253-66.

2. Shade A, McManus PS, Handelsman J. Unexpected diversity during community succession in the apple flower microbiome. MBio. 2013;4(2):e00602-12.

3. Ambika Manirajan B, Ratering S, Rusch V, Schwiertz A, Geissler□Plaum R, Cardinale M, et al. Bacterial microbiota associated with flower pollen is influenced by pollination type, and

451 shows a high degree of diversity and species□specificity. Environmental microbiology.
452 2016;18(12):5161-74.
453 4. Tucker CM, Fukami T. Environmental variability counteracts priority effects to facilitate
454 species coexistence: evidence from nectar microbes. Proceedings of the Royal Society B:
455 Biological Sciences. 2014;281(1778):20132637.
456 5. Pusey PL, Rudell DR, Curry EA, Mattheis JP. Characterization of stigma exudates in
457 aqueous extracts from apple and pear flowers. HortScience. 2008;43(5):1471-8.
458 6. Stockwell V, McLaughlin R, Henkels M, Loper J, Sugar D, Roberts R. Epiphytic
459 colonization of pear stigmas and hypanthia by bacteria during primary bloom. Phytopathology.
460 1999;89(12):1162-8.
461 7. Steven B, Huntley RB, Zeng Q. The influence of flower anatomy and apple cultivar on
462 the apple flower phytobiome. Phytobiomes. 2018;2(3):171-9.
463 8. Norelli JL, Jones AL, Aldwinckle HS. Fire blight management in the twenty-first
464 century: using new technologies that enhance host resistance in apple. Plant Disease.
465 2003;87(7):756-65.
466 9. Thomson S, Wagner A, Gouk S, editors. Rapid epiphytic colonization of apple flowers
467 and the role of insects and rain. VIII International Workshop on Fire Blight 489; 1998.
468 10. Pusey PL, Stockwell VO, Mazzola M. Epiphytic bacteria and yeasts on apple blossoms
469 and their potential as antagonists of Erwinia amylovora. Phytopathology. 2009;99(5):571-81.
470 11. Sinclair L, Osman OA, Bertilsson S, Eiler A. Microbial community composition and
471 diversity via 16S rRNA gene amplicons: evaluating the illumina platform. PloS one.
472 2015;10(2):e0116955.
473 12. Pirc M, Ravnikar M, Tomlinson J, Dreo T. Improved fireblight diagnostics using
474 quantitative real□time PCR detection of Erwinia amylovora chromosomal DNA. Plant
475 Pathology. 2009;58(5):872-81.

476 13. Cui Z, Yuan X, Yang C-H, Huntley RB, Sun W, Wang J, et al. Development of a method
477 to monitor gene expression in single bacterial cells during the interaction with plants and use to
478 study the expression of the type III secretion system in single cells of Dickeya dadantii in potato.
479 Frontiers in microbiology. 2018;9:1429.
480 14. Schloss PD, Westcott SL, Ryabin T, Hall JR, Hartmann M, Hollister EB, et al.
481 Introducing mothur: open-source, platform-independent, community-supported software for
482 describing and comparing microbial communities. Appl Environ Microbiol. 2009;75(23):7537-
483 41.
484 15. Rognes T, Flouri T, Nichols B, Quince C, Mahé F. VSEARCH: a versatile open source
485 tool for metagenomics. PeerJ. 2016;4:e2584.
486 16. Westcott SL, Schloss PD. OptiClust, an improved method for assigning amplicon-based
487 sequence data to operational taxonomic units. MSphere. 2017;2(2):e00073-17.
488 17. Quast C, Pruesse E, Yilmaz P, Gerken J, Schweer T, Yarza P, et al. The SILVA
489 ribosomal RNA gene database project: improved data processing and web-based tools. Nucleic
490 acids research. 2012;41(D1):D590-D6.
491 18. Wang Q, Garrity GM, Tiedje JM, Cole JR. Naive Bayesian classifier for rapid
492 assignment of rRNA sequences into the new bacterial taxonomy. Appl Environ Microbiol.
493 2007;73(16):5261-7.
494 19. Dixon P. VEGAN, a package of R functions for community ecology. Journal of
495 Vegetation Science. 2003;14(6):927-30.
496 20. Wickham H. ggplot2: elegant graphics for data analysis: Springer; 2016.
497 21. Berendsen RL, Pieterse CM, Bakker PA. The rhizosphere microbiome and plant health.
498 Trends in plant science. 2012;17(8):478-86.
499 22. Albrecht M, Padrón B, Bartomeus I, Traveset A. Consequences of plant invasions on
500 compartmentalization and species' roles in plant–pollinator networks. Proceedings of the Royal
501 Society B: Biological Sciences. 2014;281(1788):20140773.

502 23. Edlund AF, Swanson R, Preuss D. Pollen and stigma structure and function: the role of
503 diversity in pollination. The Plant Cell. 2004;16(suppl 1):S84-S97.
504 24. Fridman S, Izhaki I, Gerchman Y, Halpern M. Bacterial communities in floral nectar.
505 Environmental Microbiology Reports. 2012;4(1):97-104.
506 25. Yuan J, Chaparro JM, Manter DK, Zhang R, Vivanco JM, Shen Q. Roots from distinct
507 plant developmental stages are capable of rapidly selecting their own microbiome without the
508 influence of environmental and soil edaphic factors. Soil Biology and Biochemistry.
509 2015;89:206-9.
510 26. Marschner P, Neumann G, Kania A, Weiskopf L, Lieberei R. Spatial and temporal
511 dynamics of the microbial community structure in the rhizosphere of cluster roots of white lupin
512 (Lupinus albus L.). Plant and Soil. 2002;246(2):167-74.
513 27. Bardgett RD, Bowman WD, Kaufmann R, Schmidt SK. A temporal approach to linking
514 aboveground and belowground ecology. Trends in ecology & evolution. 2005;20(11):634-41.
515 28. Goldford JE, Lu N, Bajić D, Estrela S, Tikhonov M, Sanchez-Gorostiaga A, et al.
516 Emergent simplicity in microbial community assembly. Science. 2018;361(6401):469-74.
517 29. Pusey P, Stockwell V, Reardon C, Smits T, Duffy B. Antibiosis activity of Pantoea
518 agglomerans biocontrol strain E325 against Erwinia amylovora on apple flower stigmas.
519 Phytopathology. 2011;101(10):1234-41.
520 30. Herrera CM. Microclimate and individual variation in pollinators: flowering plants are
521 more than their flowers. Ecology. 1995;76(5):1516-24.
522 31. Medzhitov R, Schneider DS, Soares MP. Disease tolerance as a defense strategy.
523 Science. 2012;335(6071):936-41.
524 32. Hamdan-Partida A, González-García S, de la Rosa García E, Bustos-Martínez J.
525 Community-acquired methicillin-resistant Staphylococcus aureus can persist in the throat.
526 International Journal of Medical Microbiology. 2018;308(4):469-75.

527 33. Peacock SJ, de Silva I, Lowy FD. What determines nasal carriage of Staphylococcus
528 aureus? Trends in microbiology. 2001;9(12):605-10.
529 34. Von Eiff C, Becker K, Machka K, Stammer H, Peters G. Nasal carriage as a source of
530 Staphylococcus aureus bacteremia. New England Journal of Medicine. 2001;344(1):11-6.
531 35. Paetzold B, Willis JR, de Lima JP, Knödlseder N, Brüggemann H, Quist SR, et al. Skin
532 microbiome modulation induced by probiotic solutions. Microbiome. 2019;7(1):95.
533 36. Trosvik P, Stenseth NC, Rudi K. Convergent temporal dynamics of the human infant gut
534 microbiota. The ISME journal. 2010;4(2):151.
535 37. Shenhav L, Furman O, Briscoe L, Thompson M, Silverman JD, Mizrahi I, et al.
536 Modeling the temporal dynamics of the gut microbial community in adults and infants. PLOS
537 Computational Biology. 2019;15(6):e1006960.
538 38. Giatsis C, Sipkema D, Smidt H, Verreth J, Verdegem M. The colonization dynamics of
539 the gut microbiota in tilapia larvae. PLoS One. 2014;9(7):e103641.
540 39. Booijink CC, El□Aidy S, Rajilić□Stojanović M, Heilig HG, Troost FJ, Smidt H, et al.
541 High temporal and inter□individual variation detected in the human ileal microbiota.
542 Environmental microbiology. 2010;12(12):3213-27.
543 40. Bolnick DI, Snowberg LK, Hirsch PE, Lauber CL, Org E, Parks B, et al. Individual diet
544 has sex-dependent effects on vertebrate gut microbiota. Nature communications. 2014;5:4500.
545 41. Colman DR, Toolson EC, Takacs□Vesbach C. Do diet and taxonomy influence insect
546 gut bacterial communities? Molecular ecology. 2012;21(20):5124-37.
547 42. Turnbaugh PJ, Ley RE, Mahowald MA, Magrini V, Mardis ER, Gordon JI. An obesity-
548 associated gut microbiome with increased capacity for energy harvest. nature.
549 2006;444(7122):1027.
550 43. Mariat D, Firmesse O, Levenez F, Guimarães V, Sokol H, Doré J, et al. The
551 Firmicutes/Bacteroidetes ratio of the human microbiota changes with age. BMC microbiology.
552 2009;9(1):123.

553 44. Råberg L, Sim D, Read AF. Disentangling genetic variation for resistance and tolerance

554 to infectious diseases in animals. Science. 2007;318(5851):812-4.

555

Figure legends

Figure 1. Illustration of apple flower clusters. (**A**) An apple flower cluster at "king bloom". This is when flower clusters of the same age were tagged. (**B**) Once the surrounding flowers opened (one day after king bloom), stigmas of flowers were sampled and named as "day 1". Each sample contains stigmas collected from an individual flower. A close up photo of individual stigmas is shown in the inset. (**C**) An example showing a flower with fire blight disease and a healthy flower coexisting in the same flower cluster. (Photo courtesy: Q. Zeng)

Figure 2. Temporal dynamics in the predominant bacterial families present on stigmas of individual flowers. Each column represents a single flower. The seven most abundant families are displayed, and the category "rare" represents the sum of the remaining taxa. The relative abundance of OTU1, identified as sharing 100% sequence identity with *Erwinia amylovora*, is indicated by hatched lines. Copy numbers of *E. amylovora amsC* gene in each sample were determined by qPCR, and are displayed in the bar graphs above the stacked columns. The average DNA copies are indicated as well as the average relative abundance of OTU1. The change in *Ea* inoculated compared to water control was labeled in the brackets. Water control: flower clusters sprayed with sterile H_2O. *Ea* inoculated: flower clusters sprayed with a bacterial suspension of *E. amylovora* strain 110. Day 1-day 5 represent the number of days after petals opened during bloom.

Figure 3. (**A**) Non-metric Multidimensional Scaling (NMDS) plot displaying relationships of stigma microbial community composition in samples from water control (green) and *Ea* inoculated samples (gold). Symbols indicate stigma sample collection day. The distances were determined using the Bray-Curtis metric and the stress value of the ordination is indicated. Statistically significant differences in clustering were evaluated via the Adonis permutation test and P-values are indicated. (**B**) Comparative analysis of community diversity (Shannon index) among stigma samples. Changes in diversity over time for the water control samples (left panel) and the *Ea* inoculated samples (middle panel), respectively. The bar above day 1 and day 2 indicates the pre-treatment samples, which are the same between the panels. Overall diversity of water control samples versus *Ea* inoculated samples (far right panel). Statistically significant differences were identified by ANOVA comparisons of means, employing a post-hoc Tukey-Cramer test for multiple comparisons. Boxes labeled with different letters showed statistically significant differences (P-value <0.05).

Figure 4. (**A**) DNA copy numbers of the *Ea* specific gene *amsC* ordered by abundance in 100 flowers. The dashed line represents average copy number across the samples. (**B**) Relative abundance (%) of the two major bacterial families within *Proteobacteria* in the stigma microbiome of 100 flowers. Each column represents an individual flower. The columns are ordered by *amsC* copy number to match Fig. 4A. (**C**) OTUs within the family *Pseudomonadaceae* and (**D**) *Enterobacteriaceae.* The category "rare" represents the sum of the remaining taxa.

Figure 5. Correlations of *Ea* abundance as measured by qPCR against metrics of microbiome composition. (**A**) Relative abundance (%) of OTU1 identified as *Ea* (R^2 = 0.29, P = 0.28), (**B**) Relative abundance (%) of sequences within the *Pseudomonadaceae* family (R^2 = 0.26, P = 0.00), (**C**) community diversity (Shannon index) (R^2 = 0.02, P = 0.19), and (**D**) Number of recovered

OTUs (R^2 = 0.005, P = 0.49). The dashed line is best fit from a linear model test. RA: relative abundance.

Figure S1. Schematic diagram describing temporal dynamics and spatial distribution sampling.

Figure S2. Temporal dynamics in the predominant bacterial phyla present on stigmas of individual flowers. Each column represents a single flower and are ordered by *Ea* abundance as determined by qPCR to match Fig. 2. The five most abundant phyla are displayed, and the category "rare" represents the sum of the remaining taxa. Water control: flower clusters sprayed with sterile H_2O. *Ea* inoculated: flower clusters sprayed with a bacterial suspension of *E. amylovora* strain 110.

Figure S3. Relative abundance (%) of the four major bacterial phyla in the stigma microbiome of 100 flowers. Each column is an individual flower and are ordered by *amsC* copy number to match Fig. 4A. The five most abundant phyla are displayed, and the category "rare" represents the sum of the remaining taxa.

Figure S4. Correlational analysis in the relative abundance of OTU5 (most abundant OTU within the *Pseudomonadaceae*) against the relative abundance of *Pseudomonadaceae* (R^2 = 0.26, P = 0.00). The dashed line is best fit from a linear model test.

Day 1
Day 2
Day 3
Day 4
Day 5
Water control
Ea inoculated
DNA copy number
% of sequences
Avg = 8.0E+6
Avg% of OTU1 = 3.5
Avg = 7.5E+6
Avg% of OTU1 = 5.7
Avg = 5.7E+6
Avg% of OTU1 = 1.6
Avg = 7.4E+6
Avg% of OTU1 = 13.0
Avg = 1.5E+7
Avg of OTU1 = 24.1
Avg = 7.0E+6 (22.8%)
Avg% of OTU1 = 50.2 (30.4-fold)
Avg = 3.0E+7 (305.4%)
Avg% of OTU1 = 86.2 (5.6-fold)
Avg = 4.3E+8 (2766.7%)
Avg% of OTU1 = 94.4 (2.9-fold)
OTU1
Non-OTU1 *Enterobacteriaceae*
Pseudomonadaceae
Moraxellaceae
Beijerinckiaceae
Gammaproteobacteria_unclassified
Burkholderiaceae
Xanthomonadaceae
rare

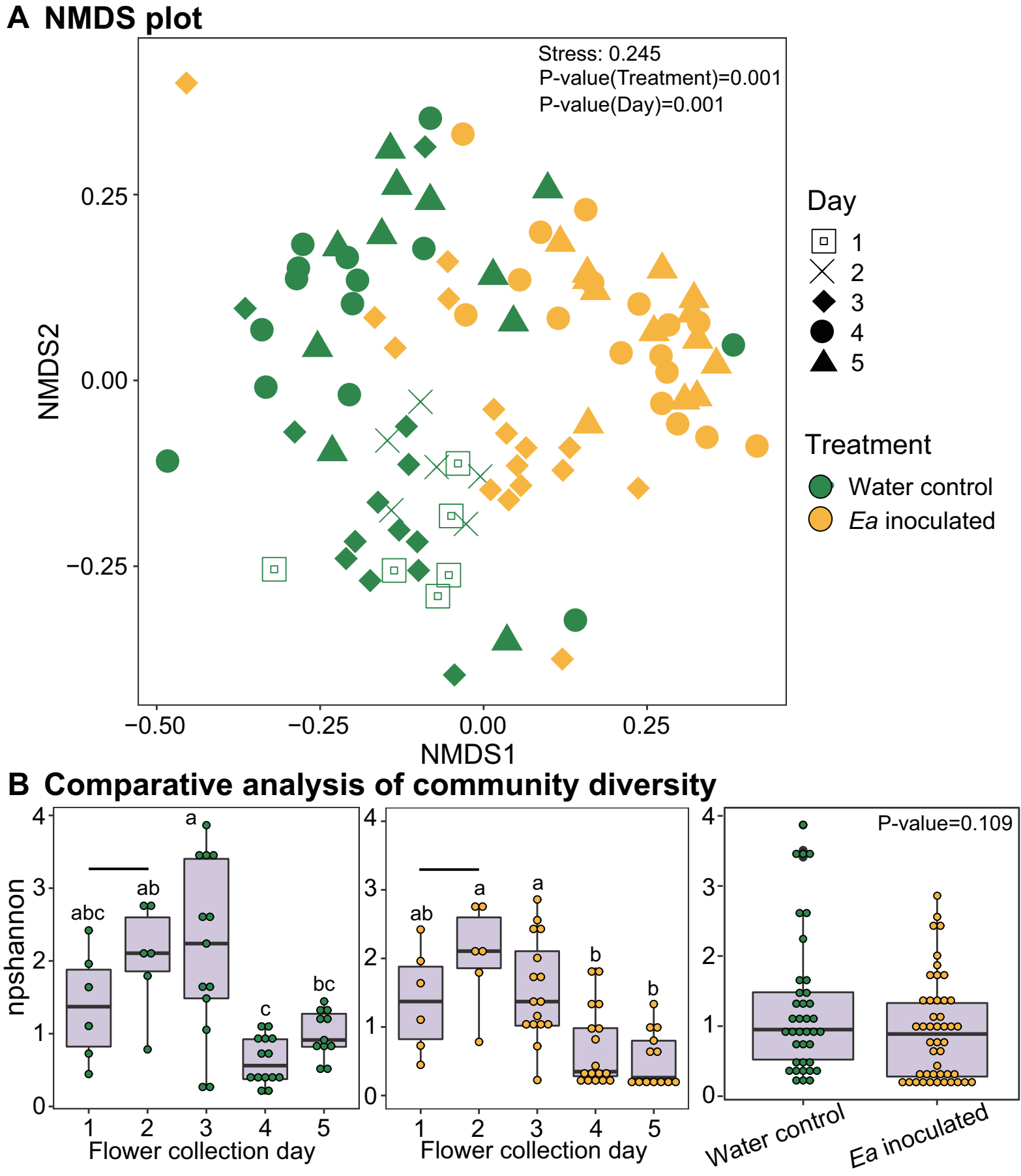
A NMDS plot
Stress: 0.245
P-value(Treatment)=0.001
P-value(Day)=0.001
NMDS2
NMDS1
0.25
0.00
−0.25
−0.50
−0.25
0.00
0.25
Day
1
2
3
4
5
Treatment
Water control
Ea inoculated
B Comparative analysis of community diversity
npshannon
abc
ab
a
c
bc
ab
a
a
b
b
P-value=0.109
Flower collection day
Flower collection day
Water control
Ea inoculated

A *E. amylovora* quantification

DNA copy number (Log10)

11
10
9
8
7
6
5
4

B Family level taxonomic bins

100
80
60
40
20
0

Enterobacteriaceae
Pseudomonadaceae
rare

% of sequences

C OTUs within *Pseudomonadaceae*

100
80
60
40
20
0

OTU4
OTU5
OTU6
OTU7
rare

D OTUs within *Enterobacteriaceae*

100
80
60
40
20
0

OTU1
OTU2
OTU3
OTU8
OTU9
OTU10
rare

Low *Ea* copy number → High *Ea* copy number

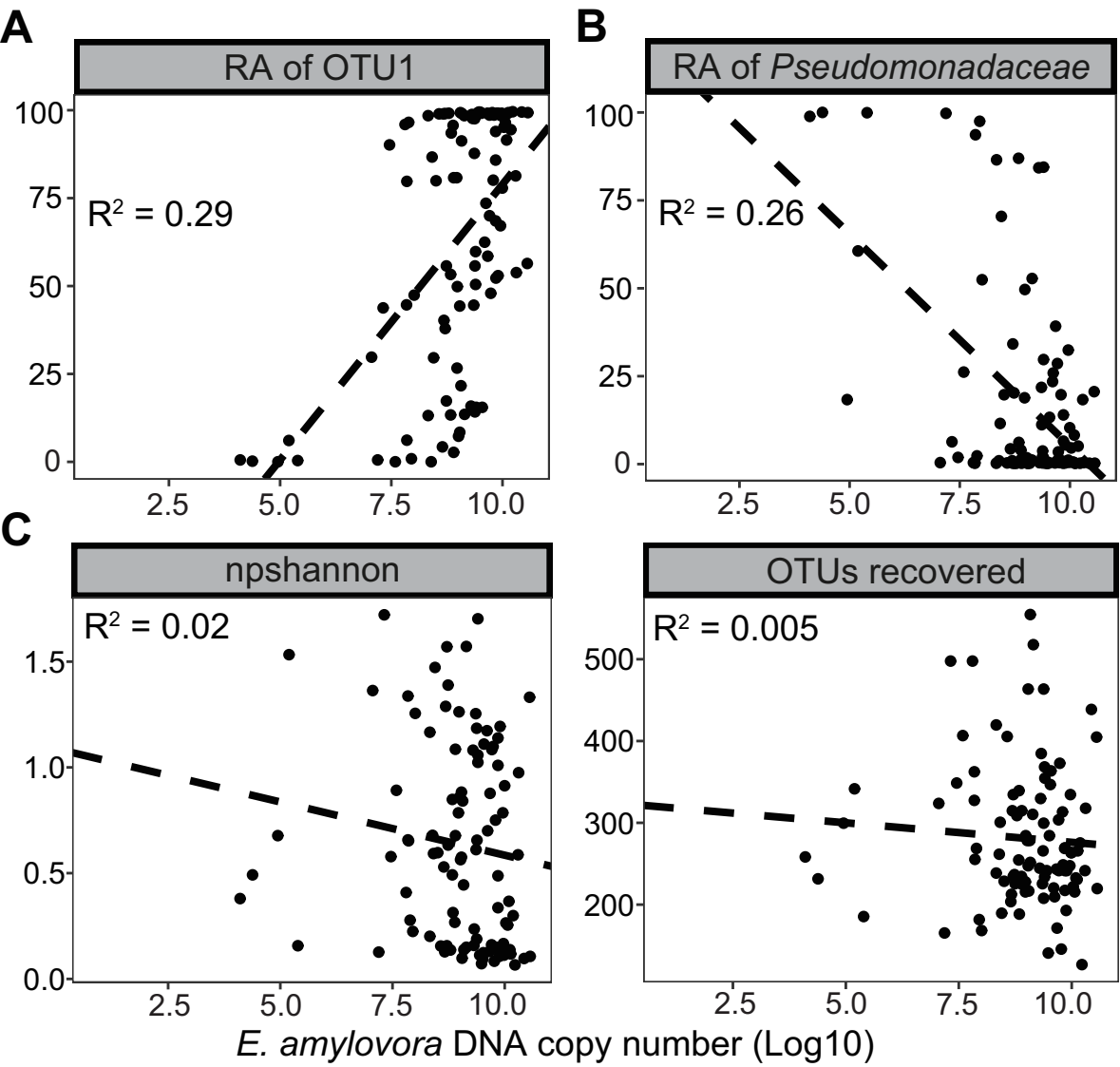
A
RA of OTU1
R² = 0.29
B
RA of Pseudomonadaceae
R² = 0.26
C
npshannon
R² = 0.02
OTUs recovered
R² = 0.005
E. amylovora DNA copy number (Log10)